ALGINATE BEADS AND EPOXY RESIN COMPOSITES AS CANDIDATES FOR MICROWAVE ABSORBERS

I. Zivkovic[1, *], C. Wandrey[2], and B. Bogicevic[3]

[1]Institute of Applied physics, University of Bern, Siedlerstrasse, 5, Bern 3012, Switzerland

[2]Institut d'Ingenierie Biologique et Institut des Sciences et Ingenierie Chimiques, Ecole Polytechnique Federale de Lausanne, EPFL-SV-IBILMRP, Station 15, CH-1015 Lausanne, Switzerland

[3]Forschungsanstalt Agroscope Liebefeld Posieux ALP, Schwarcenburgstr. 161, CH-3003 Bern, Switzerland

Abstract—This paper presents a new composite material, which is developed by mixing calcium alginate spheres with commercially available epoxies Stycas 2850 FT (s2850) and Stycast W19 (W19). The resulting composite material is examined in terms of transmission and reflection coefficients in microwave frequencies (26 to 40 GHz, 70 to 110 GHz and 300 to 320 GHz). The study reveals that the new material exhibits reflection coefficients much lower than some commercial CR absorbers from the Eccosorb group. The experimental results justify the use of the new composite material as absorber at microwave frequencies.

1. INTRODUCTION

Microwave absorbing materials attract increasingly attention because of their commercial and military use and potential. Microwave absorbers can be used as isolator from electromagnetic radiation created by different sources and devices. There exist a number of different microwave absorbing materials. They differ, for example, in composition, shape, as well as thermal and electrical behavior. Carbon nanotubes [1], carbonyl iron powder [2, 3], or steel powder [4], can be used as inclusion in such composite material.

In this work, we present a basic concept how to use calcium alginate (Ca-alg) as a component in absorbing composite mixtures.

Alginates are biopolymers extracted from brown algae. Their sodium salts are water-soluble. The interaction with divalent cations such as Ca^{2+} or Ba^{2+} yields hydrogels usually containing over 90% of water. Various technologies yield spherical hydrogels with diameters adjustable in the range of a few microns to few millimeters upon extrusion of a sodium alginate (Na-alg) solution through a needle or nozzle into a gelation bath. Such microspheres serve as containers for a multitude of materials including solids, vitamins, hormones and even living cells ([5–8]). Our idea was to encapsulate iron particles (CIP, carbonyl iron powder) into Ca-alg and subsequently to incorporate these into epoxy material. For comparison, 'empty', non-loaded Ca-alg is incorporated into epoxy. Transmission and reflection properties of such composites are investigated experimentally and numerically, and obtained results are compared with the performance of commercially available absorbers.

2. COMPOSITE PREPARATION

We prepared two types of Ca-alg, empty spheres and spheres loaded with CIP. We used a simple droplet formation process. The Na-alg solution was extruded into the gelation bath using a syringe with a thin needle diameter (0.8 mm). Attention was paid to keep sufficient distance between the needle and the bath surface in order to allow the formation of spherical droplets.

2.1. Preparation of Loaded and 'Empty' Alginate Spheres

A clear aqueous Na-alg solution (100 ml, 2%wt) was obtained by dissolving Na-alg powder (Kelton LV, lot No. 46198 Kelco, San Diego, CA, USA) under slight warming and constant mixing for 45 minutes. The 5%wt of CIP (ES type, from BASF company) is added to one part of the clear Na-alg solution and mixed.

The aqueous gelation bath contained 2%wt completely dissolved $CaCl_2$. The Na-alg solutions with and without CIP were extruded into separate gelation baths. Gelation was completed after approximately 3 min. The Ca-alg spheres with diameters in the range of 1 to 2 mm were separated from the bath by filtration.

2.2. Incorporation of Alginate Spheres into Epoxy Matrices

Both empty and loaded Ca-alg spheres were incorporated into an epoxy matrix. Epoxy resins that are used are commercially available Stycast W19 (W19) and Stycast 2850 FT (s2850) from Emerson &
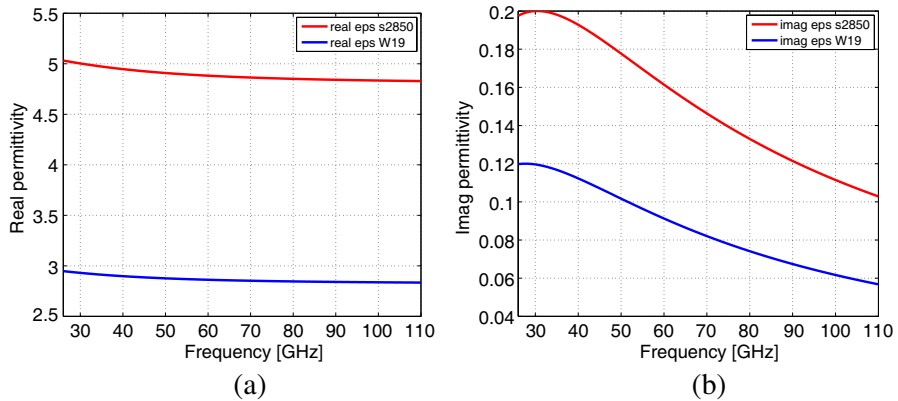
Figure 1. (a) Real and (b) imaginary part of permittivity of s2850 and W19 epoxies.

Cuming Company. The difference between the two epoxies lays in their dielectric properties. Real and imaginary parts of dielectric permittivity of both epoxies are presented in Figure 1. For s2850, higher values of both real and imaginary permittivity are obvious than for W19. Permittivity values for both epoxies are extracted from transmission measurements in 70 to 110 GHz range. The detailed procedure is described in [9]. As another difference, W19 is less viscous than s2850.

The procedure for the preparation of the composite samples is the following: 100 g of W19 is mixed with 15 g of C9 hardener. Then 10g of boron nitride powder (BN) is added and mixed to obtain a homogeneous mixture. Due to the low viscosity of W19, BN is added to increase the viscosity and to avoid the aggregation of the incorporated Ca-alg spheres at the bottom of the mold. Finally, 35 g of Ca-alg spheres are added. The mixture is poured into silicone molds and left 24 h at room temperature to cure. The same process is repeated with the CIP loaded Ca-alg spheres. The final material samples are of plane parallel circular shape and 13.3 mm thick. Two samples with Ca-alg spheres, with and without CIP, are obtained in similar way with s2850 epoxy resin. 100 g of s2850 is mixed with 4 g of C9 hardener. In that mixture 7 g of Ca-alg spheres are added. Everything is poured into silicone molds and left for 24 h at room temperature to cure. The same procedure is repeated to obtain composite with Ca-alg spheres containing CIP. These final samples are the same as with W19, plane parallel circular shape and 13.3 mm thick.

The samples that are made with W19 epoxy contain 21.9%wt of

Ca-alg spheres (sample of Ca-alg loaded with CIP has 1%wt of CIP), while samples prepared with s2850 contain 6.3%wt of Ca-alg (samples of alginate loaded with CIP has 0.25%wt of CIP).

3. MEASUREMENT RESULTS

3.1. Transmission Measurements

We performed transmission and reflection measurements on the fabricated samples. Free space transmission measurements were performed in Ka (26 to 40 GHz), W (70 to 110 GHz) and Y (320 to 360 GHz) bands. Free space measurements at lower frequencies (below 26 GHz) were not feasible because of the limited diameter of the samples. In Ka band measurements were obtained with HP 8510C Vector Network Analyzer (VNA) while in W and Y bands with an Abmm Vector Network Analyzer (Abmm VNA).

Antennas that we used are corrugated horn antennas which provide a better approximation of free space propagation at the aperture than rectangular antennas. For transmission measurements horn antennas are aligned and fabricated sample is placed on the aperture of one of the antennas. Calibration for S_{21} measurements is done with a 'through' measurement (Equation (1)).

$$S_{21\text{cal}} = \frac{S_{21\text{meas}}}{S_{21\text{through}}} \tag{1}$$

In Equation (1) $S_{21\text{cal}}$ is calibrated signal; $S_{21\text{meas}}$ is transmission parameter measured through material sample; $S_{21\text{through}}$ is through
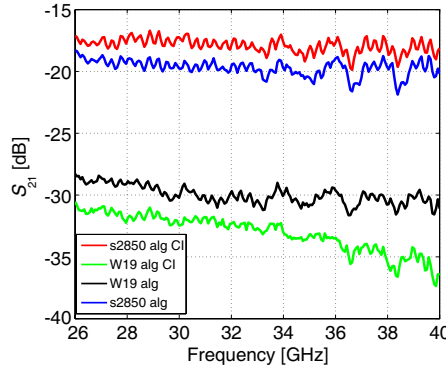

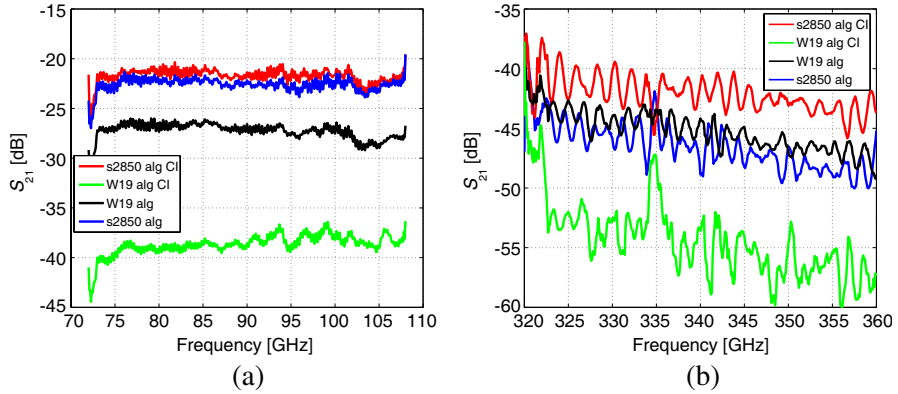**Figure 2.** Transmission measurements in Ka band for all fabricated samples.

Figure 3. Transmission measurements in (a) W and in (b) Y bands for all fabricated samples.

measurement (measured transmission without sample between transmitting and receiving antenna).

Figures 2 and 3 represent transmission measurements of all fabricated samples in the mentioned bands. In Figure 3, transmission measurement in Y band for the sample W19 with CIP loaded alginate, becomes very noisy because the dynamic range is reached.

3.2. Reflection Measurements

If we want to use the material as electromagnetic wave absorbing material then the reflection coefficient with metal backing (metal plate on the back side of sample) is of interest because it is close to the real situation. On the same samples that we performed the transmission, we performed also the reflection measurements. We placed material samples with and without metal backing at the aperture of the antenna. Antenna is connected to the VNA through directional coupler. For calibration purposes we measure the reference signal (metal plate is on the aperture of the antenna, 100% reflection) and signal when the antenna is pointed on low reflectivity pyramidal foam absorber (to calibrate directivity). Calibration of the measured reflection parameter is given by Equation (2).

$$S_{11\text{cal}} = \frac{S_{11\text{meas}} - S_{11\text{foam}}}{S_{11\text{alu}} - S_{11\text{foam}}} \tag{2}$$

In Equation (2), $S_{11\text{cal}}$ is calibrated signal; $S_{11\text{meas}}$ is measured reflection parameter of the sample; $S_{11\text{foam}}$ is measured reflection when foam absorber is on the top of antenna's aperture; $S_{11\text{alu}}$ is reference

reflection measurement, when metal is on the aperture of the antenna. Reflection measurements are performed in Ka (on VNA) and W band (on Abmm VNA), Figure 4.

3.3. Discussion of the Measurement Results

The transmission measurements show almost no frequency dependence for the measured bands. For the s2850 samples, there is no remarkable difference between samples with and without CIP. That is because of the very low CIP content (0.25%) in the composite. Similar observation is valid for the W19 samples, but only in the Ka band. In W band we can notice that the transmission of the sample that contains CIP inside the Ca-alg is around 10 dB lower than the transmission of the sample without CIP. Due to the low total content of CIP of only 1%, one could conclude that an increase of the CIP amount inside the Ca-alg will result in further decrease of S_{21}, which refers to an increase of the absorption of the composite material.

Figure 3(b) presents the transmission measurements at very high frequencies. At these frequencies scattering plays significant role beside absorption since Ca-alg sphere diameter is comparable to the wavelength. For the sample W19 with CIP loaded alginate, the measurements become very noisy because the dynamic range is reached.

In Figure 4(a), only the reflection measurements with and without metal backing on W19 composites are performed (s2850 composite
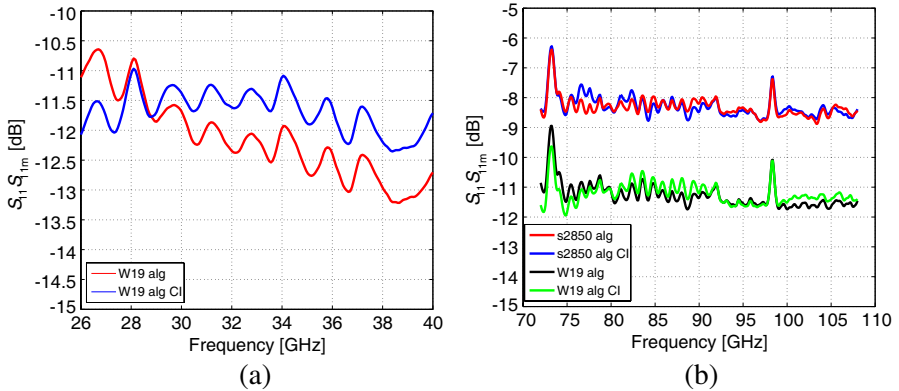

Figure 4. Reflection measurements of the W19 alginate sample in Ka band with and without metal backing (a) and measured reflection at W band of all fabricated samples with and without metal backing (b).

samples were too small for the measurements). There is no difference between the measured reflection with and without metal backing. The reason for this is that for the given thickness and frequency the absorption in the sample is high so that the incident signal does not 'see' metal backing or the second sample/air interface. In Figure 4(b), the measured reflections of all composites in W band are presented. Reflections from the W19 composites are ∼ 6 dB lower than from the s2850 samples.

In the Sections 4.2 and 4.3, we will present and compare simulated reflection and transmission coefficients of the synthesized samples of different thicknesses as well as of some commercially available absorbers.

4. EFFECTIVE PERMITTIVITY OF COMPOSITES AND SIMULATED REFLECTION COEFFICIENTS

4.1. Extraction of Effective Permittivity

At high frequencies magnetic materials exhibits only dielectric properties, which means that the material is characterized only with permittivity values. We will extract effective permittivity of the composites (s2850 and alginate, W19 and alginate and W19, alginate and CIP) in W band as follows. We assume that in the microwave region, synthesized composites have one relaxation frequency and for that reason the frequency dependent permittivity of the composite is represented with Debye relaxation model [9]. This model is incorporated into Fresnell equations based algorithm. Simulated transmission parameters are fitted with measured transmission data
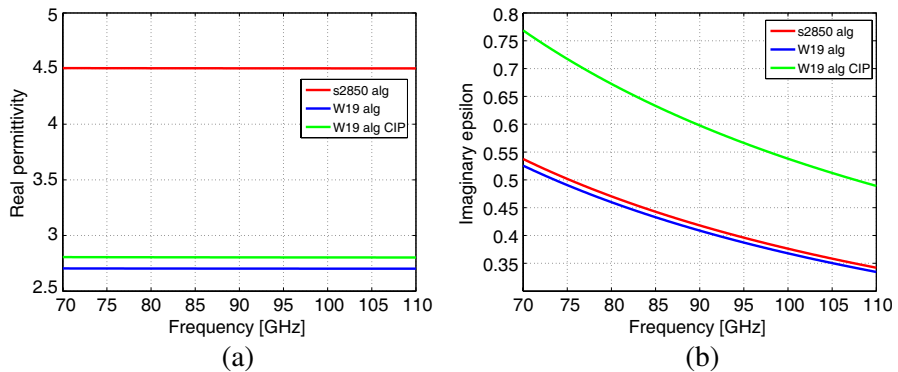

Figure 5. Extracted effective permittivity of all fabricated samples.

(both in amplitude and phase) with least square fitting routine. In this way, unknown parameters of Debye model for frequency dependent permittivity are extracted. Procedure for fitting and permittivity extraction is described in more details in [9].

In Figure 5, real and imaginary frequency dependent permittivity of synthesized composites are presented. The highest value of the real part of permittivity is for the s2850 alginate composite, which is expected because s2850 epoxy itself has higher real permittivity than W19 (Figure 1). Imaginary part of permittivity is connected to the losses in material. From Figure 5, the highest imaginary part is for W19 alginate and CIP composite. If we directly compare W19 alginate and W19 alginate with CIP, 1% difference of CIP content between the two composites introduces significant loss, which leads to the conclusion that higher inclusion of the CIP can even more increase composites absorption.

4.2. Simulated Reflection Coefficients and Comparison with the Commercial Absorbers

The extracted effective permittivity is used for the simulation of reflection coefficients for the samples of different thicknesses, with and without metal backing. Reflection coefficient simulations are performed by using algorithm based on Fresnell equations. Simulated reflections of the fabricated samples as well as of commercially available absorbers from CR Eccosorb group (CR114 and CRS117) are presented in Figures 6 to 10. The values for the frequency dependent permittivity
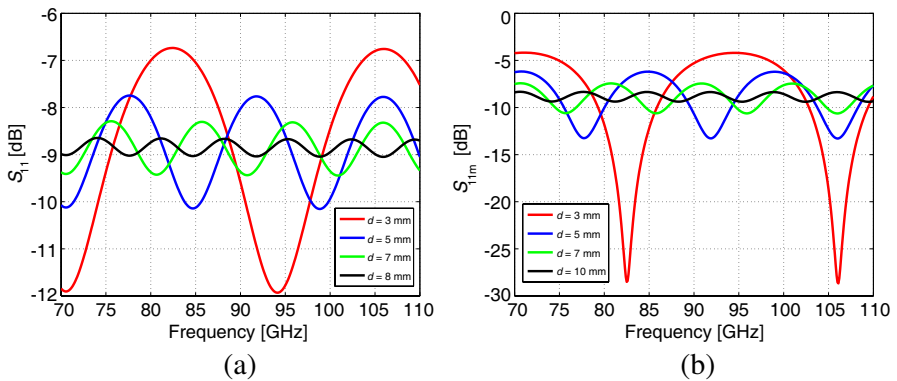

Figure 6. Simulated reflection coefficients of s2850 alginate composites (with and without metal backing) in W band for four different sample thicknesses — 3, 5, 7 and 10 mm.

of CR114 and CRS117 are taken from [9].

Simulations are performed for all samples in four different thicknesses 3, 5, 7 and 10 mm. By changing thickness of the sample, resonance can be tuned. In the case when metal is placed on the back side of sample and reflection is measured (or simulated), there is constructive and destructive interference. Because of that, reflection is at some frequencies high and at the others low. For some thickness value, incident signal does not 'see' the back side (the second
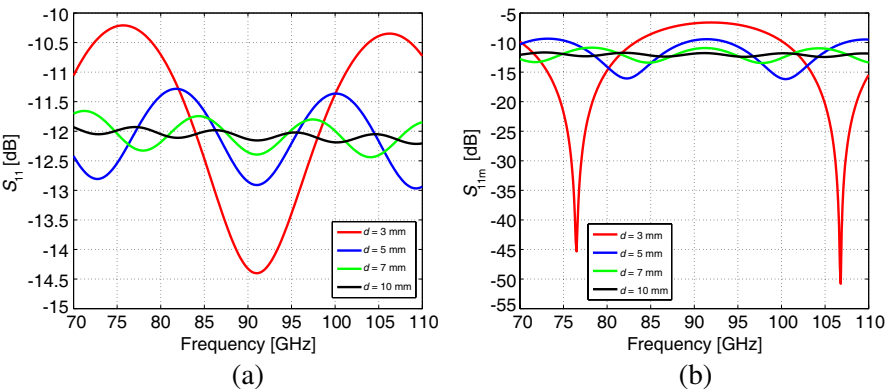

Figure 7. Simulated reflection coefficients of W19 alginate composite (with and without metal backing) in W band for four different sample thicknesses — 3, 5, 7 and 10 mm.
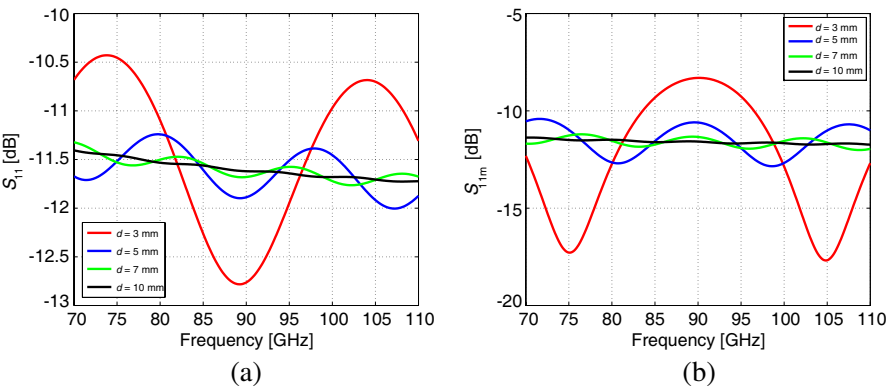

Figure 8. Simulated reflection coefficients of W19 alginate and CIP composite (with and without metal backing) in W band for four different sample thicknesses — 3, 5, 7 and 10 mm.
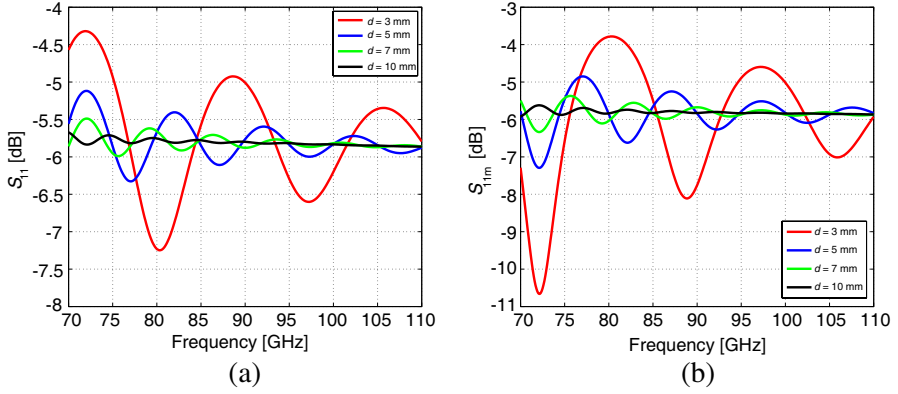
Figure 9. Simulated reflection coefficients of CR114 material (with and without metal backing) in W band for four different sample thicknesses — 3, 5, 7 and 10 mm.

Figure 10. Simulated reflection coefficients of CRS117 material (with and without metal backing) in W band for four different sample thicknesses — 3, 5, 7 and 10 mm.
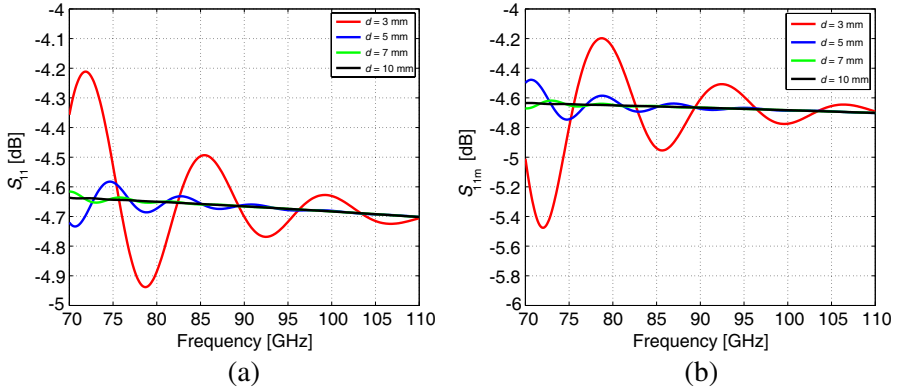
sample/air interface for S_{11} or metal backing for S_{11m}). In that case measured or simulated reflections with and without metal backing are the same.

In Figures 6 to 10, for the lowest simulated sample thicknesses we can observe resonance features. The resonances for W19 alginate and W19 alginate and CIP samples are at the same frequencies. The deepest resonances are for the W19 alginate sample. The reason is by introducing of CIP loading, absorption of the composite increases

(that is seen in transmission measurements in W band, Figure 3(a)) but at the same time permittivity increases and mismatch at air/sample interface becomes higher which produces higher reflection. In all simulations, for the sample thickness of 10 mm, reflections with and without metal backing are the same and frequency independent. That is because only the reflection from the first air/sample interface exists. From simulations, the lowest reflection has composite of W19 and alginate. Compared to the reflection of CR114, for example, it is 6 dB lower.
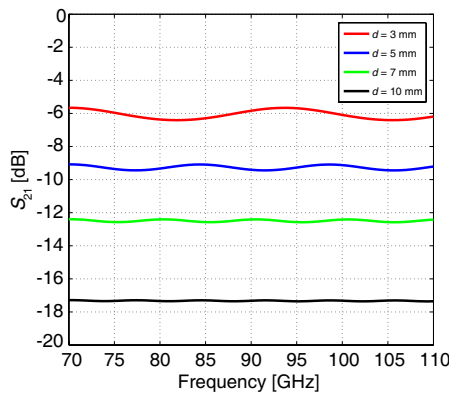

Figure 11. Simulated transmission coefficients of s2850 alginate material in W band for four different sample thicknesses — 3, 5, 7 and 10 mm.
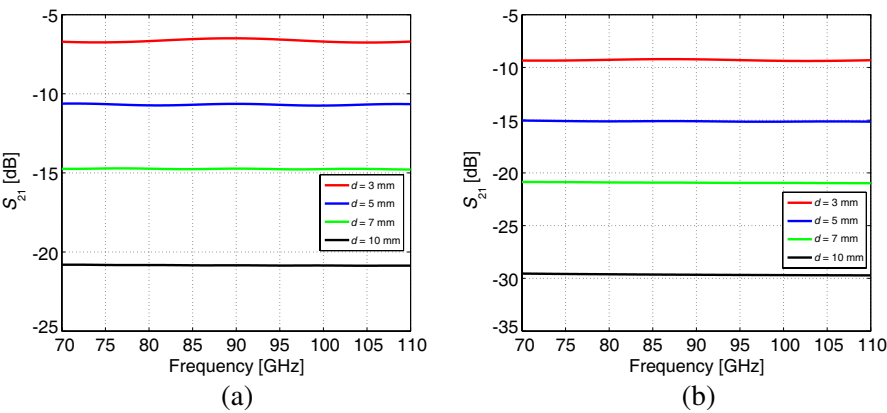

Figure 12. Simulated transmission coefficients of W19 alginate (a) and W19 alginate and CIP (b) materials in W band for four different sample thicknesses — 3, 5, 7 and 10 mm.
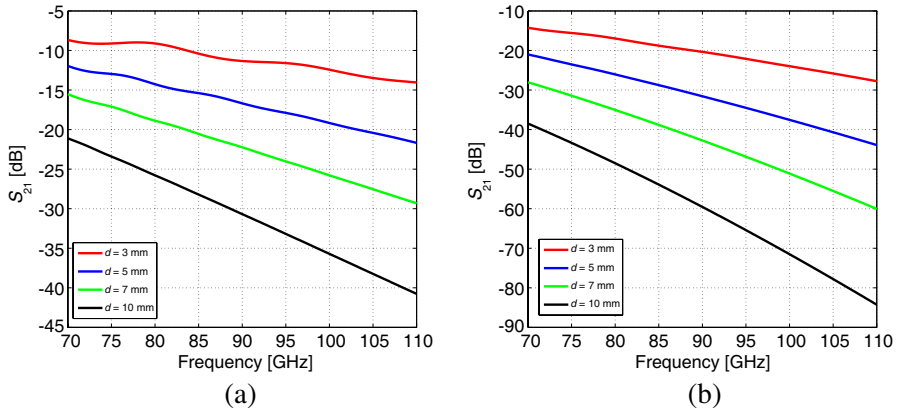
Figure 13. Simulated transmission coefficients of CR114 and CRS117 materials in W band for four different sample thicknesses — 3, 5, 7 and 10 mm.

4.3. Simulated Transmission Coefficients and Comparison with the Commercial Absorbers

Same as in simulations of the reflection coefficients, extracted effective permittivity is used for the simulation of transmission coefficients for the samples of different thicknesses. Transmission coefficient simulations are performed by using algorithm based on Fresnell equations. Simulated transmissions of the fabricated samples as well as of commercially available absorbers from CR Eccosorb group (CR114 and CRS117) are presented in Figures 11 to 13. The values for the frequency dependent permittivity of CR114 and CRS117 are taken from [9].

From the simulated S_{21} can be concluded that when sample thickness increases, transmission decreases for all materials. In Figure 12, simulated transmissions of the W19 alginate with and without CIP loading are presented. Transmission is significantly lower in the case of W19 alginate loaded with CIP material because of additional losses introduced by CIP loading.

Simulated transmission coefficients of the fabricated samples that contain alginate spheres, are frequency independent in W band frequencies. That is not a case for the simulated transmissions of CR114 and CRS117 materials, where S_{21} decreases when frequency increases. This is because of the difference in frequency dependance of permittivities of examined materials.

5. LOSS MECHANISMS — ABSORPTION AND SCATTERING

Absorption and scattering are loss mechanisms that occur simultaneously. Which one will be dominant depends on the chemical composition of the particles, their size, shape, surrounding material and on the other side on polarization state and frequency of the incident beam. Term extinction includes both absorption and scattering. To approximately predict magnitude of absorption and scattering that happen in the composite, we calculate Mie efficiencies.

Mie efficiencies are dimensionless numbers and efficiencies that we calculate are Qext (extinction efficiency), Qabs (absorption efficiency) and Qsca (scattering efficiency) [10]. Equations from which we calculate Mie efficiencies are 3 to 7. Detailed equations as well as MATLAB code for Mie efficiencies calculations are in [11].

$$Q_{ext} = Q_{abs} + Q_{sca} \tag{3}$$

$$Q_{sca} = \frac{2}{x^2} \sum (2n+1) \left(|a_n|^2 + |b_n|^2 \right) \tag{4}$$

$$Q_{ext} = \frac{2}{x^2} \sum (2n+1) \mathrm{Re}(a_n + b_n) \tag{5}$$

$$a_n = \frac{m^2 j_n(mx)[xj_n(x)]' - j_n(x)[mxj_n(mx)]'}{m^2 j_n(mx)[xh_n^{(1)}(x)]' - h_n^{(1)}(x)[mxj_n(mx)]'} \tag{6}$$

$$b_n = \frac{j_n(mx)[xj_n(x)]' - j_n(x)[mxj_n(mx)]'}{j_n(mx)[xh_n^{(1)}(x)]' - h_n^{(1)}(x)[mxj_n(mx)]'} \tag{7}$$

where m is refractive index of the sphere; $x = \frac{2\pi a}{\lambda}$ is the size parameter depending on the ratio between the sphere radius a and wavelength; a is radius of sphere; j_n and h_n are spherical Bessel functions; primes $'$ are the first derivatives with respect to the arguments.

In Figure 14, the calculated Mie efficiencies for the sphere of different radii are presented. We do not know frequency dependent permittivity of alginate. Because it contains over 90% of water, in Mie efficiencies calculation as permittivity of sphere we used frequency dependent permittivity of water (Equation (8), [12]).

$$\varepsilon = 4.9 + \frac{75.2}{1 + \frac{jf}{99}} \tag{8}$$

where ε is frequency dependent permittivity of water; f is frequency in GHz.

Calculations are performed up to 200 GHz frequency because at higher frequencies the second resonance will influence water
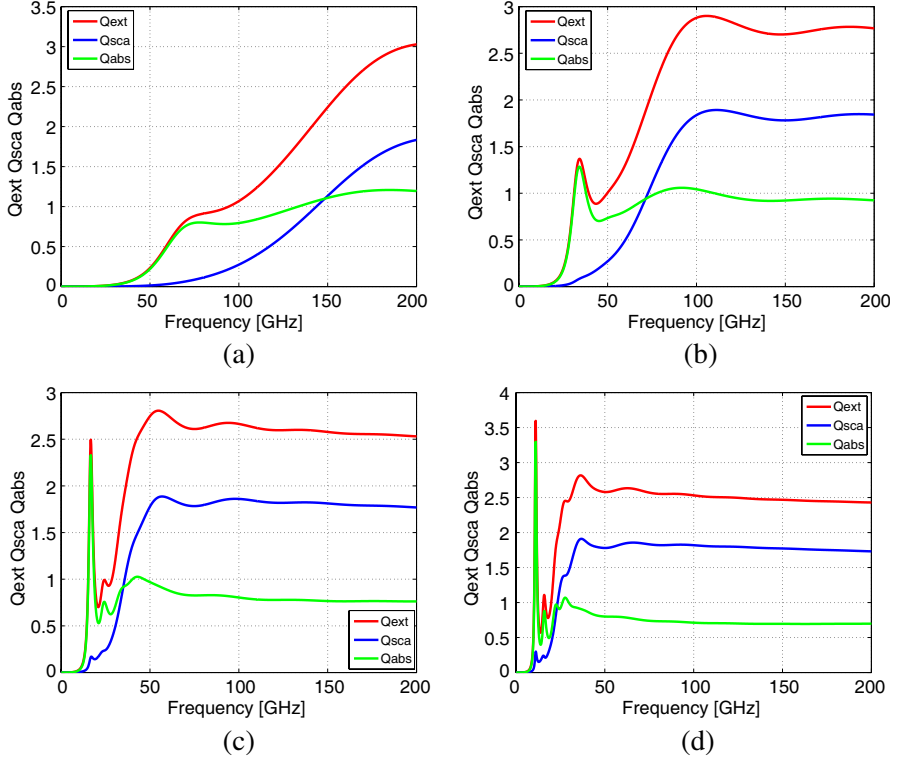
Figure 14. Simulated Mie scattering efficiencies for the sphere radius
(a) $a = 0.25\,\mathrm{mm}$, (b) $a = 0.5\,\mathrm{mm}$, (c) $a = 1\,\mathrm{mm}$ and (d) $a = 1.5\,\mathrm{mm}$.

permittivity and representation of permittivity with Equation (8), will
not be valid anymore.

Absorption is dominant over scattering at higher frequencies for
the smaller sphere radius. By increasing sphere radius, domination
of absorption over scattering shifts to the lower frequencies. From
Figure 14, at frequencies where the absorption is dominant over
scattering we can observe peak of extinction coefficient. The peak
is more pronounced when the sphere size increases. Observed peak
in extinction coefficient can cause deep resonance in transmission
measurements at the same frequency.

Radii of our alginate particles are between 0.5 and 1 mm (diameter
is from 1 to 2 mm) and simulations in Figures 14(b) and (c) correspond
to these radii. From the simulations can be concluded that in W band,
scattering is dominant loss mechanism over absorption.

6. CONCLUSIONS

In this paper we proposed a procedure to prepare composite materials of Ca-alg spheres and commercially available epoxies. Characterization results of a series of samples are presented. The measurements revealed that the reflection from the fabricated samples is constant over the examined frequency range and comparable with reflections of some commercially available absorbing materials. What is interesting to note are differences in the measured transmissions in the W band of the samples made from W19 epoxy. The only difference between the samples is that one contains 1%wt of CIP, which obviously introduces losses. This leads to the conclusion that if we incorporate more CIP into the Ca-alg, losses in the composite will increase.

Effective permittivity of the composites are extracted and reflection and transmission coefficients are simulated. We observe that proposed W19 alginate composite exhibits the lowest reflection compared to the other composites as well as to the commercially available absorbers. That is very important characteristics for the application of material as absorber of electromagnetic radiation.

Future studies will focus on the characteristics of composite material containing variable volume fractions of Ca-alg spheres of different sizes, 'empty' and loaded with CIP incorporated into epoxy resin.

REFERENCES

1. Zhao, D. L. and Z. M. Shen, "Microwave absorbing property and complex permittivity and permeability of epoxy composites containing Ni-coated and Ag filled carbon nanotubes," *Composite Science and Technology*, Vol. 68, 2902–2908, 2008.

2. Yang, R. B. and W. F. Liang, "Microwave properties of high aspect ratio carbonyl iron/epoxy absorbers," *Journal of Applied Physics*, Vol. 109, 07A311, 2011.

3. Gama, A. M. and M. C. Rezende, "Complex permeability and permittivity variation of carbonyl iron rubber in the frequency range of 2 to 18 GHz," *Journal of Aerospace Technology and Management*, Vol. 2, No. 1, 2010.

4. Wollack, E. J., et al., "Electromagnetic and thermal properties of a conductively loaded epoxy," *International Journal of Infrared and Millimeter Waves*, Vol. 29, 51–61, 2008.

5. Khalil, A. H. and E. H. Mansour, "Alginate encapsulated bifidobacteria survival in mayonnaise," *Journal of Food Science*, Vol. 63, 702–705, 1998.

6. Sultana, K., et al., "Encapsulation of probiotic bacteria with alginate starch and evaluation of survival in simulated gastrointestinal conditions and in yoghurt," *International Journal of Food Microbiology*, Vol. 62, 47–55, 2000.

7. Wang, N., et al., "Alginate encapsulation technology supports embryonic stem cells differentiation into insulin-producing cells," *Journal of Biotechnology*, Vol. 144, No. 4, 304–312, 2009.

8. Zimmermann, H., et al., "Towards a medically approved technology for alginate based microcapsules allowing long-term immunoisolated transplantation," *Journal of materials science: Materials in Medicine*, Vol. 16, No. 6, 491–501, 2005.

9. Zivkovic, I. and A. Murk, "Characterization of magnetically loaded microwave absorbers," *Progress In Electromagnetics Research B*, Vol. 33, 277–289, 2011.

10. Bohren, C. F. and D. R. Hufman, *Absorption and Scattering of Light by Small Particles*, Wiley-VCH, Weinheim, 2004.

11. Mätzler, C., "MATLAB functions for mie scattering and absorption," IAP Research Report, No. 2002-08, Institut für Angewandte Physik, Universität Bern, 2002.

12. Sihvola, A., *Electromagnetic Mixing Formulas and Applications*, *IEE Electromagnetic Waves Series*, 47, TJ International, UK, 1999.